Int J CARS (2009) 4:299–306
DOI 10.1007/s11548-009-0295-0

ORIGINAL ARTICLE

Automated analysis of breast parenchymal patterns in whole breast ultrasound images: preliminary experience

Yuji Ikedo · Takako Morita · Daisuke Fukuoka · Takeshi Hara · Gobert Lee · Hiroshi Fujita · Etsuo Takada · Tokiko Endo

Received: 24 September 2008 / Accepted: 18 February 2009 / Published online: 14 March 2009

Abstract
Purpose A computerized classification scheme to recognize breast parenchymal patterns in whole breast ultrasound (US) images was developed. A preliminary evaluation of the system performance was performed.
Methods Breast parenchymal patterns were classified into three categories: mottled pattern (MP), intermediate pattern (IP), and atrophic pattern (AP). Each classification was defined as proposed by an experienced physician. A total of 281 image features were extracted from a volume of interest which was automatically segmented. Canonical discriminant analysis with stepwise feature selection was employed for the classification of the parenchymal patterns.
Results The classification scheme accuracy was computed to be 83.3% (10/12 cases) in MP cases, 91.7% (22/24 cases) in IP cases, 92.9% (13/14 cases) in AP cases, and 90.0% (45/50 cases) in all the cases.
Conclusions The feasibility of an automated ultrasonography classifier for parenchymal patterns was demonstrated with promising results in whole breast US images.

Keywords Ultrasonographic breast parenchymal pattern · Whole breast ultrasound · Computerized classification · Canonical discriminant analysis

Y. Ikedo (✉) · T. Hara · G. Lee · H. Fujita
Department of Intelligent Image Information,
Division of Regeneration and Advanced Medical Sciences,
Graduate School of Medicine, Gifu University,
Yanagido, Gifu, Japan
e-mail: ikedo@fjt.info.gifu-u.ac.jp

T. Morita
Department of Mammary Gland, Chunichi Hospital,
Naka-ku, Nagoya, Japan

D. Fukuoka
Technology Education, Faculty of Education, Gifu University,
Yanagido, Gifu, Japan

E. Takada
Center of Medical Ultrasonics, Dokkyo Medical University School of Medicine, Shimotsuga-gun, Tochigi, Japan

T. Endo
Department of Radiology, National Hospital Organization Nagoya Medical Center, Naka-ku, Nagoya, Japan

Introduction

Breast cancer is one of the malignancies with high incidence rate in the world. In Japan, breast has been the most commonly involved site among female Japanese cancer patients since 1996 [1]. Mammography is an effective screening method for early detection of breast cancer. It is shown to help to reduce mortality [2,3]. Biennial screening mammography has been recommended by the Japanese Ministry of Health, Labour and Welfare for all women over the age of 40. However, mammography is less effective in dense breasts because lesions might be obscured by dense fibroglandular tissues in the breast [4–6]. In contrast, ultrasonography may be particularly useful for detection of the lesions in such dense breasts. Actually, breast cancer screening with ultrasonography has started in some areas of Japan because Japanese women tend to have relatively denser breasts than their counterparts in Western countries and the breast cancer incidence rate is high for women aged 40–59 years in Japan. The effectiveness of combined screening with ultrasonography and mammography has also been reported [7–9].

Ultrasonography using a conventional hand-held probe is an operator-dependent examination which potentially has following problems: (1) Examination accuracy depends on

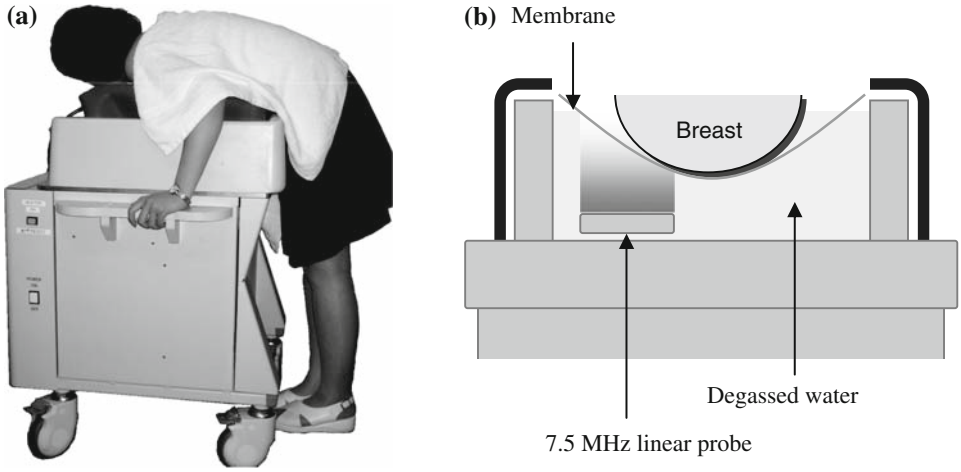

Fig. 1 Whole breast ultrasound scanner ASU-1004. **a** A patient positions her breast on the scanner. **b** Structure of the scanner (*cross sectional view*). The scanner has a water tank with a linear probe and a membrane

operator's skills. (2) Part of a breast may not been scanned due to error. (3) It is difficult for double reading. (4) It is also difficult to directly compare with mammography. Recently, some automated whole breast ultrasound (US) scanners have been developed for breast cancer screening [10–12]. These instruments automatically scan entire breast without leaving any part of the breast unscanned and they do not produce operator-dependent subjective images but objective images. Therefore, these scanners are probably useful in the screening and breast cancer screening with ultrasonography would be increased by promoting widespread use of whole breast US scanners.

The Japanese mammography guideline categorizes mammographic parenchymal patterns as fatty, scattered fibroglandular, heterogeneously dense, and extremely dense based on visual assessment. The assessment indicates the degree of risk where the lesions are obscured by normal mammary gland tissues, i.e., reliability of diagnosis. Moreover, it is also an index for recommending another examination such as ultrasonography. Such assessment is not described in the Japanese breast ultrasonography guideline because radiologists examine the patient and interpret the images at the same time during breast cancer screening with conventional ultrasonography. However, in case of screening with automated whole breast US scanners, radiologists can interpret US images after examination similar to mammography. As a result, the assessment of ultrasonographic parenchymal patterns may be needed in whole breast US images. In addition, such assessment may be useful as a marker of breast cancer risk because it have been reported that the risk for women with increased mammographic parenchymal density is at a four to sixfold higher than women with primarily fatty breasts [13–18].

While visual assessment of mammographic parenchymal patterns is poorly reproducible due to the subjective assessment [17] and extensive training is required for improving the concordance rate, computerized methods can yield objective measures. Many researchers have developed the computerized methods for the assessment of mammographic patterns [18–22]. In case of whole breast US images, computerized methods for assessing parenchymal patterns will probably be useful. Chang et al. [23] proposed two methods where whole breast US images were automatically classified into mammographic grades. However, there have been no reports on the computerized analysis of parenchymal patterns in whole breast US images except for our initial experimental work [24]. Thus, the purpose of our study was to design a method for the classification of breast parenchymal patterns in whole breast US images and to perform a preliminary evaluation of the performance of this method. We improved the performance of the classification by the addition of image features and the selection of useful features.

Materials and methods

Database

A data set of whole breast US cases was collected by the researcher (T.M.). Patients were scanned with an automated whole breast US scanner ASU-1004 (ALOKA Co., Ltd.) [10], as shown in Fig. 1, which had a 7.5 MHz 6 cm linear transducer (US probe) immersed in a water tank and moved mechanically. A patient positions her one breast at a time on a membrane covering the water tank, and the instrument scans her entire breast in three overlapping runs. A whole breast slice image (axial plane) was generated from three original images by using an integration algorithm proposed in our previous work for computerized detection of masses in whole breast US images [25]. The whole breast slice image consisted of 167 slice images with 1-mm slice intervals, and the width and depth of each slice image were 611 and 469 pixels, respectively. The images had a gray-level resolution of 8 bits.

In this preliminary study, three categories of ultrasonographic parenchymal patterns, namely, mottled pattern (MP),

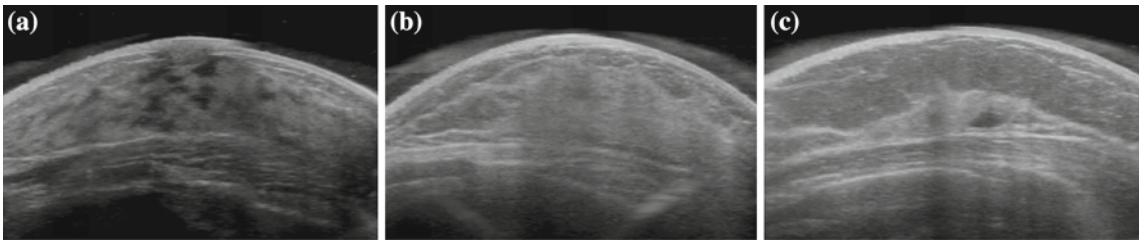

Fig. 2 Ultrasonographic parenchymal patterns in each category. **a** Mottled pattern (MP). **b** Intermediate pattern (IP). **c** Atrophic pattern (AP)

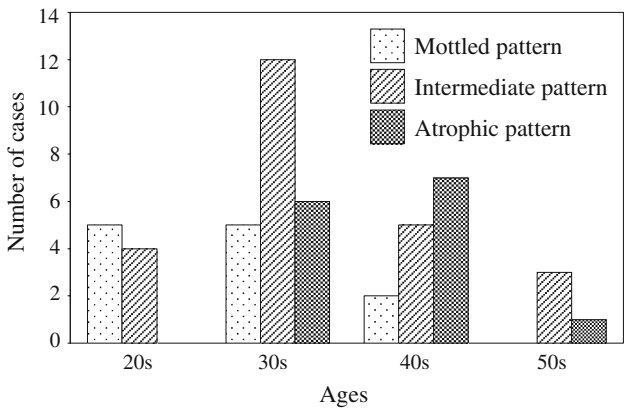

Fig. 3 Distribution of each pattern according to age in the 50 whole breast ultrasound cases

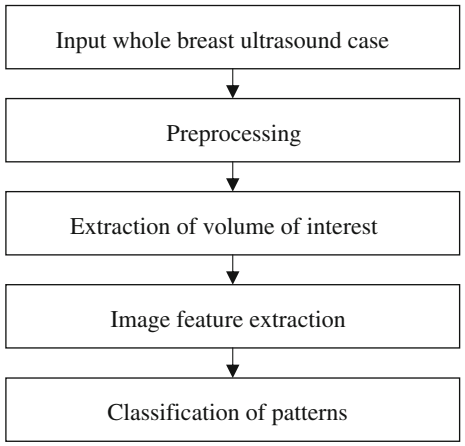

Fig. 4 Overall computerized scheme for classification of parenchymal patterns in whole breast ultrasound images

intermediate pattern (IP), and atrophic pattern (AP), were defined and proposed based on breast parenchymal conditions by a Japan Association of Breast and Thyroid Sonology (JABTS) certified physician (T.M.) who has 18 years of experience in breast ultrasonography. Examples of each pattern are shown in Fig. 2. In the case of MP, many small hypoechoic regions are included in a mammary gland because the gland contains large amount of milk. In the case of AP, while a lot of fat tissues are contained in a breast, mammary gland tissues are fewer than other cases because the gland has atrophied. The IP case is an intermediate case between MP and AP cases and many mammary gland tissues are observed in the image.

The whole breast US cases obtained 50 patients aged 24–59 years (mean 37.1 years, median 35 years) were used for this study. The 50 experimental cases were categorized into 12 MP, 24 IP, and 14 AP by the same physician (T.M.) who proposed those categories. The distribution of age in each pattern of 50 cases is shown in Fig. 3. MP was more frequent in the 20s and 30s, and IP and AP were more frequent in the 30s and 40s, respectively. Although, it was expected for AP in the 50s to be more frequent than other patterns in the 50s, IP was more frequent. Besides, the AP was more frequent in the 40s, and less frequent in the 50s. These were attributed to the fact that the number of cases in 50s was extremely few.

Computerized analysis of ultrasonographic parenchymal patterns

Overview

The developed scheme for the classification of parenchymal patterns in whole breast US images includes several major steps: preprocessing, extraction of volume of interest (VOI), image feature extraction, and classification, as shown in Fig. 4. A preprocessing which consisted of noise reduction and normalization of gray levels was performed after generating a whole breast US image. Then image features were extracted from a VOI which was automatically defined in the entire breast volume image. Finally, we classified the parenchymal patterns based on statistical methods and extracted image features.

Preprocessing

Many noises such as impulse and speckle noises are generally included in US images, which are caused by the interference effects between overlapping echoes. Furthermore, image brightness also varies due to adjustment of the gain control for an US system. In this step, we produced three images which were used for various processes in subse-

quent steps. First, we generated an image f_1 from an original whole breast image by applying a median filter for reduction of impulse noises. An image f_2, brightness normalized, and an image f_3, brightness normalized after speckle noise reduction, were produced from the image f_1. A histogram equalization technique was adopted for normalizing image brightness, and an anisotropic diffusion filter [26] was applied for the reduction of speckle noises. The images f_1 and f_2 were used in the image feature extraction step because various texture features affected by speckle noises were useful for the classification of ultrasonographic parenchymal patterns. In contrast, the most noise-reduced image f_3 was used in the VOI extraction procedure because the segmentation algorithm was easily influenced by noises.

Extraction of volume of interest

The whole breast US images generally included artifacts, pectoral muscle, ribs, and abdominal regions except mammary gland and fat tissues. Therefore, we extracted image features only from VOIs in the breast images to avoid preferably effects of there regions. The VOI was defined in the breast region behind the nipple position in an image. As mammary glands extend from the nipple to the entire breast, the VOI usually includes mammary gland tissues. The point with the maximum value of y axis in a breast volume was determined as the nipple position $N = (n_x, n_y, n_z)$, where xy and z axes are defined in axial plane and in the slice direction, respectively. The breast volume was segmented from the image f_3 with our proposed method [25], as shown in Fig. 5. The VOI was empirically defined as $n_x - 95 \leq x \leq n_x + 95$, $n_y - 76 \leq y \leq n_y, n_z - 25 \leq z \leq n_z + 25$ within the breast volume.

Image feature extraction

Four groups of features based on the absolute value of the gray levels, gray-level histogram analysis, small hypoechoic regions, and textures were extracted from a VOI. Six features based on the absolute value of the gray levels included the average gray-level AVG, the standard deviation of the gray levels SD, and various gray-level thresholds that yield 5, 30, 70, and 95% of the area under the gray-level histogram of the VOI in the image f_2. The gray-level threshold features indicated difference of distribution of gray-level histogram [21], and the trend of the distribution was different from each breast parenchymal pattern in the images. Accordingly, the features were employed in this study. The 5, 30, 70, and 95% gray-level threshold features were denoted as GT_5, GT_{30}, GT_{70}, and GT_{95}, respectively. The four features based on gray-level histogram analysis included the skewness, the kurtosis, the balance 1, and the balance 2 of the histogram in the image f_2. These histogram features can be

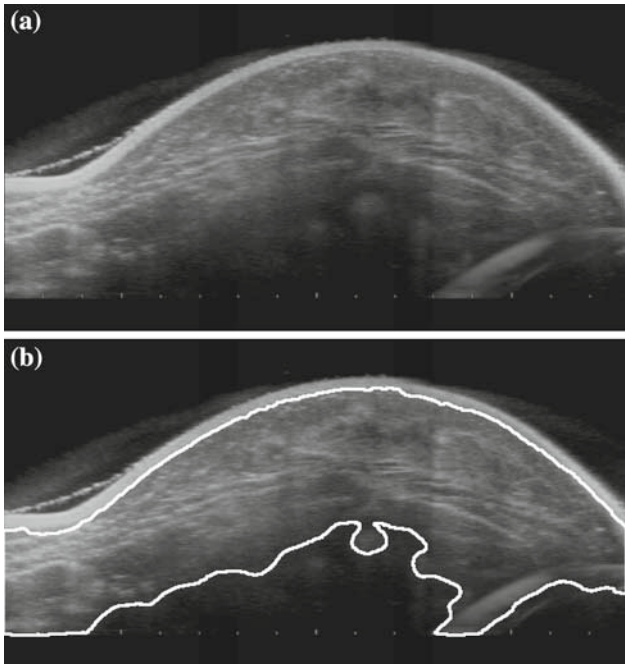

Fig. 5 Breast volume segmented from a whole breast ultrasound images. **a** Original whole breast slice image. **b** Breast volume. *Solid line* shows the contour of a breast volume

used to quantify the ratio of pixels with high gray-level values to those with low gray-level values relative to the mean. The skewness S and kurtosis K were given by

$$S = \frac{\sum_{i=0}^{255} (i-\mu)^3 p(i)}{\sigma^3},$$

$$K = \frac{\sum_{i=0}^{255} (i-\mu)^4 p(i)}{\sigma^4},$$

$$\mu = \sum_{i=0}^{255} i p(i),$$

$$\sigma^2 = \sum_{i=0}^{255} (i-\mu)^2 p(i),$$

where $p(i)$ is the normalized gray-level histogram value of gray-level value i [27]. μ and σ^2 are the average gray level and the variance of gray levels, respectively. The balance 1 B_1 and balance 2 B_2 were measured at different thresholds of the gray-level histogram to quantify the balances of the histogram [21], which were defined as

$$B_1 = \frac{GT_{95} - AVG}{AVG - GT_5},$$

$$B_2 = \frac{GT_{70} - AVG}{AVG - GT_{30}}.$$

The feature based on small hypoechoic regions was extracted from an image f_1 by use of a black top-hat transformation

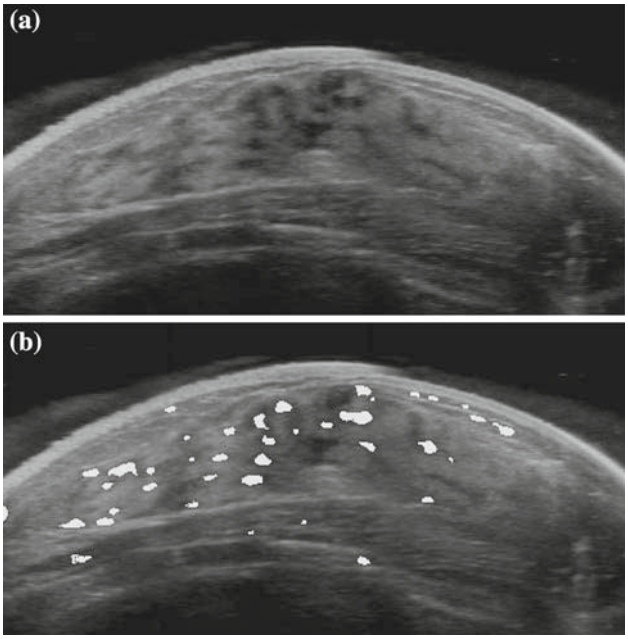

Fig. 6 Small hypoechoic regions **a** original image including small hypoechoic regions. **b** Segmented regions with a black top-hat transformation and gray-level thresholding (*white color*: segmented regions)

and gray-level thresholding, as shown in Fig. 6a. The black top-hat transformation is a gray-scale morphological operation implemented by subtracting an original image from the morphological closing image. We first applied the black top-hat transformation to the image f_1. Following this, small hypoechoic regions were segmented with gray-level thresholding technique, as shown in Fig. 6b. This feature was defined as the number of the segmented regions per unit area.

Six Haralick's texture features, i.e., energy (ENG), contrast (CNT), correlation (CRR), variance (VAR), entropy (EPY), and local homogeneity (LHG), were measured from gray level co-occurrence matrix (GLCM) [28] generated from a slice on an axial plane of a VOI. The GLCMs were computed at three different gray levels ($g = 128$, 64, and 32), five different pixel-pair distances ($d = 1, 2, 3, 4$, and 5 mm), and three different directions ($\theta = 0°$, 45°, and 90°) in the image f_2. Thus, 270 texture features were extracted in each GLCM. However, each texture feature was obtained by averaging the corresponding feature values over all slices of the VOI.

Classification of parenchymal patterns

Canonical discriminant analysis was employed for the classification of parenchymal patterns into three categories, and stepwise feature selection [21] was used to select useful features from 281 computer-extracted features. This procedure was accomplished into two steps. First, the stepwise feature selection was performed to identify useful features.

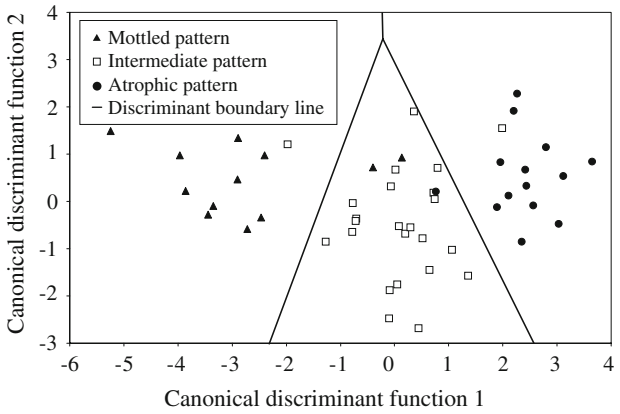

Fig. 7 Distribution of canonical discriminant scores of all 50 whole breast ultrasound cases and the discriminant boundary lines in resubstitution method

Second, coefficient of each feature variable in each discriminant function was determined by use of the selected features. In this study, two discriminant functions formulated by a linear combination of the feature variables were created to achieve maximum separation between the three categories. The stepwise procedure was based on Wilks' lambda defined as the ratio of within-group variance to the total variance and correlation coefficient of each feature.

Results

Because of the limited database available for this preliminary study, a resubstitution method was employed to evaluate the classification scheme. This method uses the same data set, first for training and then for testing. In the stepwise feature selection procedure that designs two discriminant functions, the following seven features were selected from the computer-extracted features: gray-level threshold feature GT_{95}, number of small hypoechoic regions, CRR with $g = 128$, $d = 4$, $\theta = 45$, LHG with $g = 128$, $d = 5$, $\theta = 90$, VAR with $g = 64$, $d = 5$, $\theta = 0$, EPY with $g = 64$, $d = 5$, $\theta = 90$, and CNT with $g = 32$, $d = 3$, $\theta = 45$. Figure 7 shows the distribution of the canonical discriminant scores and the discriminant boundary lines. Table 1 presents the performance of the computerized classification compared with the classification by the physician. The accuracies of the computerized classification scheme in this preliminary study were 83.3% (10/12 cases) in MP cases, 91.7% (22/24 cases) in IP cases, 92.9% (13/14 cases) in AP cases, and 90.0% (45/50 cases) in total case.

We also evaluated the performance of the classification scheme by employing leave-one-out method using the seven image features selected by the stepwise feature selection. The accuracies were 83.3% (10/12 cases) in MP cases, 83.3% (20/24 cases) in IP cases, 85.7% (12/14 cases) in AP cases, and 84.0% (42/50 cases) in total case, as shown in Table 2.

Table 1 Performance of computerized classification scheme in resubstitution method

	Computerized classification				
	Category (cases)			Accuracy (%)	
	MP	IP	AP	By category	Total
Radiologist classification					
MP	10	2	0	83.3 (10/12)	
IP	1	22	1	91.7 (22/24)	90.0 (45/50)
AP	0	1	13	92.9 (13/14)	

Table 2 Performance of computerized classification scheme in leave-one-out method

	Computerized classification				
	Category (cases)			Accuracy (%)	
	MP	IP	AP	By category	Total
Radiologist classification					
MP	10	2	0	83.3 (10/12)	
IP	1	20	3	83.3 (20/24)	84.0 (42/50)
AP	0	2	12	85.7 (12/14)	

Discussion

In this preliminary study, we used the canonical discriminant analysis and the stepwise feature selection with 281 features extracted from VOIs in whole breast US cases for the classification of breast parenchymal patterns. Although a small database was used for the evaluation, the results showed the usefulness of the proposed scheme and demonstrated the feasibility of our approach to the development of the analysis system. For a more precise evaluation, however, we need to evaluate the performance of the scheme with a cross-validation test using a larger database because the results of this study may have been biased toward the specific data set used.

One IP case was classified as category MP in resubstitution method because it included small hypoechoic regions such as MP cases, as shown in Fig. 8. These heterogeneous hypoechoic regions were not due to milk including mammary gland, but these were due to artifact like posterior attenuation caused by the nipple. In addition, the volume behind the nipple generally involved several tissues except mammary gland and fat, such as milk duct and Cooper's ligament. To improve the performance, therefore, it is necessary to develop an automated method for segmentation of tissues (skin, fat, mammary gland, etc.) in whole breast US images and then use only the mammary gland and fat volume for the classification of parenchymal patterns. Besides it is also to be expected overcoming the posterior attenuation by improving the US scanner.

Although, we used the canonical discriminant analysis as a classifier in this study, it is necessary to compare the classifier with other well-established classification algorithms for the selection of an appropriate classifier for the system. The classification performance might be improved through the use of other classifier such as an artificial neural network and a clustering algorithm.

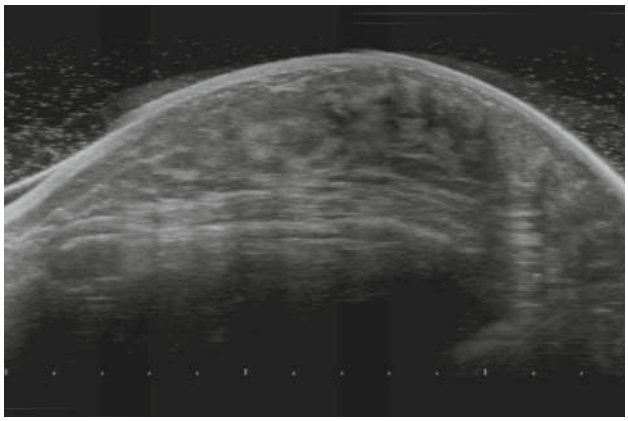

Fig. 8 Example of miss classified cases. The whole breast slice image of IP case was classified as MP case

The breast cancer risk is estimated higher for women with MP and IP breasts than AP breasts because women with mammographic dense breast tissues are grouped into higher risk [15–18]. We expect that in the future, this system for classification of breast parenchymal patterns may be applied to a computer-aided diagnosis (CAD) system for classification of breast masses and breast cancer risk estimation system. Therefore, we will improve this scheme using a larger database and the segmentation of breast tissues.

Conclusion

We developed an automated method for the classification of breast parenchymal patterns in whole breast US images into three categories and performed a preliminary evaluation of the performance of this method. The extracted image features from volume of behind the nipple and the canonical discriminant analysis with stepwise feature selection were useful for the classification of the patterns. In the future work, we need to improve the proposed scheme and evaluate the robustness of the method with a larger database.

Acknowledgments The authors are grateful to Yoshikazu Uchiyama Ph.D. for his useful discussion. The authors also thank the member of Fujita Laboratory at Gifu University for their helpful advice. This work was supported in part by a grant for the Knowledge Cluster Gifu Ogaki, referred as the "Robotics Advanced Medical Cluster", from the Ministry of Education, Culture, Sports, Science and Technology, Japan.

References

1. Minami Y, Tsubono Y, Nishino Y, Ohuchi N, Shibuya D, Hisamichi S (2004) The increase of female breast cancer incidence in Japan: emergence of birth cohort effect. Int J Cancer 108:901–906. doi:10.1002/ijc.11661
2. Fletcher SW, Black W, Harris R, Rimer BK, Shapiro S (1993) Report of the international workshop on screening for breast cancer. J Natl Cancer Inst 85:1644–1656. doi:10.1093/jnci/85.20.1644
3. Kerlikowske K, Grady D, Rubin SM, Sandrock C, Ernster VL (1995) Efficacy of screening mammography. A meta-analysis. JAMA 273:149–154. doi:10.1001/jama.273.2.149
4. Zonderland HM, Coerkamp EG, Van de Vijver MJ, Van Voorthuisen AE (1999) Diagnosis of breast cancer: contribution of US as an adjunct to mammography. Radiology 213:413–422
5. Rosenberg RD, Hunt WC, Williamson MR, Gilliland FD, Wiest PW, Kelsey CA, Key CR, Linver MN (1998) Effects of age, breast density, ethnicity, and estrogen replacement therapy on screening mammographic sensitivity and cancer stage at diagnosis: review of 183,134 screening mammograms in Albuquerque, New Mexico. Radiology 209: 511–518
6. Soo MS, Rosen EL, Baker JA, Vo TT, Boyd BA (2001) Negative predictive value of sonography with mammography in patients with palpable breast lesions. AJR Am J Roentgenol 177:1167–1170
7. Berg WA, Blume JD, Cormack JB, Mendelson EB, Lehrer D, Böhm-Vélez M, Pisano ED, Jong RA, Evans WP, Morton MJ, Mahoney MC, Larsen LH, Barr RG, Farria D, Marques HS, Boparai K (2008) Combined screening with ultrasound and mammography vs mammography alone in women at elevated risk of breast cancer. JAMA 299:2151–2163. doi:10.1001/jama.299.18.2151
8. Morikubo H (2005) Breast cancer screening by palpation, ultrasound, and mammography. In: Ueno E, Shiina T, Kubota M, Sawai K (eds) Research and development in breast ultrasound. Springer, Tokyo pp 159–162
9. Kolb TM, Lichy J, Newhouse JH (2002) Comparison of the performance of screening mammography, physical examination, and breast US and evaluation of factors that influence them: an analysis of 27,825 patient evaluations. Radiology 225:165–175. doi:10.1148/radiol.2251011667
10. Takada E, Ikedo Y, Fukuoka D, Hara T, Fujita H, Endo T, Morita T (2007) Semi-automatic ultrasonic full-breast scanner and computer-assisted detection system for breast cancer mass screenings. In: Emelianov SY, McAleavey SA (eds) Proceedings of SPIE medical Imaging 2007: ultrasonic imaging and signal processing, San Diego, CA, February 2007, pp 651310-1–651310-8
11. Chou YH, Tiu CM, Chen J, Chang RF (2007) Automated full-field breast ultrasonography: the past and the present. J Med Ultrasound 15:31–44. doi:10.1016/S0929-6441(08)60022-3
12. Duric N, Littrup P, Babkin A, Chambers D, Azevedo S, Kalinin A, Pevzner R, Tokarev M, Holsapple E, Rama O, Duncan R (2005) Development of ultrasound tomography for breast imaging: technical assessment. Med Phys 32:1375–1386. doi:10.1118/1.1897463
13. Blend R, Rideout DF, Kaizer L, Shannon P, Tudor-Roberts B, Boyd NF (1995) Parenchymal patterns of the breast defined by real time ultrasound. Eur J Cancer Prev 4:293–298. doi:10.1097/00008469-199508000-00004
14. Kaizer L, Fishell EK, Hunt JW, Foster FS, Boyd NF (1988) Ultrasonographically defined parenchymal patterns of the breast: relationship to mammographic patterns and other risk factors for breast cancer. Br J Radiol 61:118–124
15. Byng JW, Boyed NF, Fishell E, Jong RA, Yaffe MJ (1994) The quantitative analysis of mammographic densities. Phys Med Biol 39:1629–1638. doi:10.1088/0031-9155/39/10/008
16. Brisson J, Morrison AS, Khalid N (1980) Mammographic parenchymal features and breast cancer in the breast cancer detection demonstration project. J Natl Cancer Inst 80:1534–1540. doi:10.1093/jnci/80.19.1534
17. Boyd NF, O'Sullivan BO, Fishell E, Simor I, Cooke G (1984) Mammographic patterns and breast cancer risk: methodologic standards and contradictory results. J Natl Cancer Inst 72:1253–1259
18. Wolfe J (1976) Breast patterns as an index of risk for developing breast cancer. AJR Am J Roentgenol 126:1130–1139
19. Tahoces PG, Correa J, Souto M, Gomez L, Vidal JJ (1995) Computer-assisted diagnosis: the classification of mammographic breast parenchymal patterns. Phys Med Biol 40:103–117. doi:10.1088/0031-9155/40/1/010
20. Byng JW, Boyd NF, Fishell E, Jong RA, Yaffe MJ (1996) Automated analysis of mammographic densities. Phys Med Biol 41:909–923. doi:10.1088/0031-9155/41/5/007
21. Huo Z, Giger ML, Wolverton DE, Zhong W, Cumming S, Olopade OI (2000) Computerized analysis of mammographic parenchymal patterns for breast cancer risk assessment: feature selection. Med Phys 27:4–12. doi:10.1118/1.598851
22. Matsubara T, Yamasaki D, Kato M, Hara T, Fujita H, Iwase T, Endo T (2001) An automated classification scheme for mammograms based on amount and distribution of fibroglandular breast tissue density. In: Lemke HU, Vannier MW, Inamura K, Farman AG, Doi K (eds) Proceedings of the 15th international congress and exhibition on computer assisted radiology and surgery (CARS 2001), Berlin, Germany, June 2001. Elsevier Science, Amsterdam, pp 515–520
23. Chang RF, Chang-Chien KC, Takada E, Suri JS, Moon WK, Wu JHK, Cho N, Wang YF, Chen DR (2006) Breast density analysis in 3-D whole breast ultrasound images. In: Proceedings of the 28th IEEE EMBS annual international conference of the IEEE engineering in medicine and biology society (EMBS), New York City, USA, August 2006, pp 2795–2798
24. Ikedo Y, Morita T, Fukuoka D, Hara T, Fujita H, Takada E, Endo T (2008) Computerized classification of mammary gland patterns in whole breast ultrasound images. In: Proceedings of the 9th international workshop, IWDM 2008, Tucson, AZ, July 2008, pp 188–195
25. Ikedo Y, Fukuoka D, Hara T, Fujita H, Takada E, Endo T, Morita T (2007) Development of a fully automatic scheme for detection of masses in whole breast ultrasound images. Med Phys 34:4378–4388. doi:10.1118/1.2795825
26. Perona P, Malik J (1990) Scale-space and edge detection using anisotropic diffusion. IEEE Trans Pattern Anal Mach Intell 12:629–639. doi:10.1109/34.56205

27. Pitas I (2000) Texture description. In: Digital image processing algorithms and applications. Wiley Interscience, New York, pp 303–317

28. Haralick RM, Shanmugam K, Dinstein I (1973) Textural features for image classification. IEEE Trans Syst Man Cybern 3:610–621. doi:10.1109/TSMC.1973.4309314